Jurnal Teknologi

Full Paper

CO_2 REFORMING OF METHANE OVER NI SUPPORTED ON MESOSTRUCTURED SILICA NANOPARTICLES (NI/MSN): EFFECT OF NI LOADING

Siti Munirah Sidik[a], Aishah Abdul Jalil[a,b*], Sugeng Triwahyono[c], Umi Aisah Asli[a,b]

[a]Department of Chemical Engineering, Faculty of Chemical and Energy Engineering, Universiti Teknologi Malaysia, 81310 UTM Johor Bahru, Johor, Malaysia
[b]Centre of Hydrogen Energy, Institute of Future Energy, Universiti Teknologi Malaysia, 81310 UTM Johor Bahru, Johor, Malaysia
[c]Department of Chemistry, Faculty of Science, Universiti Teknologi Malaysia, 81310 UTM Johor Bahru, Johor, Malaysia

Article history
Received
19 May 2015
Received in revised form
24 March 2016
Accepted
1 May 2016

*Corresponding author
aishah@cheme.utm.my

Graphical abstract

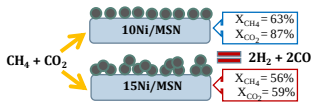

Abstract

A series of Ni incorporated Mesostructured Silica Nanoparticles (MSN) were prepared by physical mixing method. Electrolyzed nickel oxide was used as the Ni precursor. The N_2 adsorption-desorption and X-Ray diffraction (XRD) analyses evidenced that the increase in Ni loading decreased the surface area and crystallinity, and increased Ni particle size in the catalyst, respectively. The activity of CO_2 reforming of CH_4 followed the order of 10Ni/MSN > 15Ni/MSN > 5Ni/MSN > MSN. The highest activity was achieved by 10Ni/MSN with the CH_4 and CO_2 conversion of 63.4% and 87.2 %, respectively. The results indicated that the presence of a suitable Ni amount in MSN was beneficial to achieve high catalytic activity due to its effect on the amount of active metal sites available for the reaction. Thus, the electrolyzed nickel oxide precursor and Ni/MSN catalyst prepared by electrochemical method and physical mixing synthesis has a potential to be utilized in CO_2 reforming of CH_4.

Keywords: Nickel, MSN, CO_2, CH_4 reforming, loading

Abstrak

Satu siri Ni digabungkan dengan Silika Nanopartikel Berstruktur-meso (MSN) telah disediakan melalui kaedah percampuran fizikal. Nikel oksida yang telah dielektrolisis digunakan sebagai prekursor Ni. Analisis-analisis penjerapan-penyahjerapan N_2 dan pembelauan X-Ray (XRD) masing-masing membuktikan bahawa peningkatan muatan Ni menurunkan luas permukaan dan penghabluran, serta meningkatkan saiz zarah Ni dalam pemangkin. Aktiviti reformasi CH_4 dengan CO_2 adalah mengikut susunan: 10Ni/MSN > 15Ni/MSN > 5Ni/MSN > MSN. Aktiviti tertinggi telah dicapai oleh 10Ni/MSN dengan 63.4% penukaran CH_4 dan 87.2 % penukaran CO_2. Hasil kajian mendapati bahawa kehadiran jumlan Ni yang sesuai di dalam MSN adalah bermanfaat untuk mencapai aktiviti yang tinggi, disebabkan oleh kesannya keatas jumlah tapak logam aktif untuk tindak balas. Dengan itu, precursor nikel oksida dan pemangkin Ni/MSN yang disediakan dengan menggunakan kaedah elektrokimia dan kaedah sintesis pencampuran fizikal mempunyai potensi untuk digunakan dalam reformasi CH_4 dengan CO_2.

Kata kunci: Nikel, MSN, CO_2, reformasi CH_4, muatan

1.0 INTRODUCTION

Concerns about the depletion of petroleum reserves and consideration on the chemical recycling of CO_2 to fuels/chemicals warrant increasing attention for the catalytic process of CO_2 reforming of CH_4, also known as dry reforming of CH_4 [1]. This process attracted considerable attention from the industrial and environmental standpoints due to simultaneous utilization and reduction of two major greenhouse gases into more valuable synthesis gas, as represented in Equation1 below:

$$CH_4 + CO_2 \rightarrow 2H_2 + 2CO \quad (1)$$

This process offers several advantages, such as produce a lower H_2/CO ratio than those available from steam reforming and partial oxidation of methane, which is preferred for the synthesis of valuable oxygenated chemicals and long-chain hydrocarbons [2]. In the previous studies, numerous materials such as supported Ni, Co, Ru, Rh, Ir and Pt are commonly considered to be active catalysts towards this process [3-4]. Although noble metal catalysts show excellent activity, yet their low availability and high price make them unsuitable for the extensive industrial application [5]. Recently, Ni has become an ideal candidate as the catalyst due to its high activity, inherent availability and low cost [6]. However, Ni based catalysts are more incline to suffer from carbon deposition and thermal sintering of the active centers, finally causing the deactivation of the catalysts and plugging of the reactor.

The catalytic activity and stability of Ni based catalyst are affected by many factors such as nickel loading, promoters, supports, catalyst preparation procedures, and experimental conditions [7]. In this study, the effect of Ni loading on catalytic behaviors of Ni catalysts are focused on, since the Ni loading significantly affects the dispersion of Ni active sites on support. Generally, the metal species tend to be highly dispersed across support at low metal loadings, while the metal particles tend to aggregates at high metal loading, forming large particles in size. However, an optimum of nickel loading exists over the different supports [8].

Understanding this relationship can help researchers to understand dispersion-activity relationship and prepare active and stable Ni catalysts. Ni supported on mesoporous silica has been investigated for heterogeneous catalysis due to its high surface area and its ability to facilitate high metal dispersion [9]. In this work, recently developed mesostructured silica nanoparticles (MSN) was selected as the support due to high surface area and its basic feature [10]. The structural properties of Ni/MSN were characterized using N_2 adsorption-desorption, X-Ray diffraction (XRD) and Field Emission Scanning Electron Microscopy (FESEM). The catalytic performance of Ni/MSN catalysts were tested for CO_2 reforming of CH_4.

2.0 METHODOLOGY

2.1 Preparation of Catalysts

MSN was prepared by co-condensation and sol-gel method as previously reported [11]. In brief, the cetyl-trimethylammonium bromide (CTAB, Merck), ethylene glycol (EG, Merck)–and ammonium (NH_4OH, QRec) solution were dissolved in 700 mL of double distilled water with the following mole composition of CTAB:EG:NH_4OH:H_2O=0.0032:0.2: 0.2:0.1. After vigorous stirring for about 30 min at 323 K, 1.2 mmol tetraethylorthosilicate (TEOS, Merck) and 1 mmol 3-aminopropyl triethoxysilane (APTES, Merck) were added to the clear mixture to give a white suspension solution. This solution was then stirred for another 2 h at 353 K, and the as-synthesized MSN sample collected by centrifugation at 4,000 rpm. The as-synthesized MSN were dried at 373 K and calcined at 823 K for 3 h to form surfactant-free MSN. The NiO nanoparticles were prepared using electrochemical method as reported in the literature [12-14]. After electrolysis, the mixture was impregnated, oven dried overnight at 378 K, and calcined at 823 K for 3h to yield a black powder NiO. Then, a required amount of NiO was physically mixed with MSN, and calcined at 823 K for 3h to obtain 5, 10, and 15 wt% of Ni/MSN.

2.2 Characterization of Catalysts

Nitrogen (N_2) adsorption-desorption isotherms were used to determine the textural properties at liquid nitrogen temperatures using a Micromeritics ASAP 2010 instrument. The Brunnauer-Emmett-Teller (BET) and Barret-Joyner-Halenda (BJH) methods were used to calculate the surface area and pore distribution of the catalysts. Prior to measurement, all of the catalysts were outgassed at 383 K for 3 h before being subjected to N_2 adsorption at 77 K. The crystalline structure of the catalysts was determined with X-ray diffraction (XRD) recorded on powder diffractometer (Bruker AdvanceD8, 40 kV, 40 mA) using a Cu Ka radiation source in the range of 2θ= 1.5-80°. The Ni crystallite size was calculated by means of the Scherrer equation:

$$D_{NiO} = \frac{0.9\,\lambda}{\beta \cos\theta} \quad (2)$$

where λ is the X-ray wavelength corresponding to Cu-Ka radiation (0.15406 nm), β is the broadening (in radians) of the nickel (20 0) reflection and θ is the angle of diffraction corresponding to peak broadening. The morphological properties of MSN and Ni/MSN catalysts were examined by field emission scanning electron microscopy (JSM-6300F FESEM).

2.3 Catalytic Testing

The catalytic testing was carried out over CO_2 reforming of CH_4 in a fixed-bed, continuous flow reactor (Scheme 1) at 750 °C. Prior to the reaction, 0.2 g of the

catalyst was charged into an ID 4 mm quartz tube, and then it was subjected to O_2 treatment (O_2= 50 mL/min) at 800 °C for 1 h, followed by H_2 reduction (H_2= 50 mL/min) at 800 °C for 3 h. Then, the reactor was cooling down to a reaction temperature under N_2 stream. A dose of CO_2 (10 mL/ min) and CH_4 (10 mL/min) was passed over the activated catalyst.

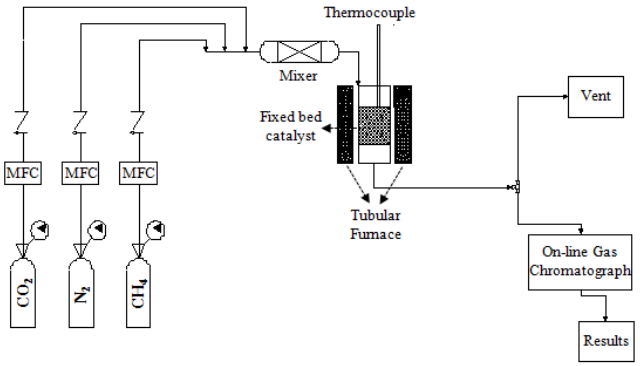

Scheme 1 Schematic equipment of continuous flow fixed-bed reactor

The products were analyzed using online 6090N Agilent Gas Chromatograph equipped with Carboxen 1010 packed column and TCD detector. The conversion of methane, X_{CH_4} and carbon dioxide, X_{CO_2} were calculated according to the following terms:

$$X_{CH_4} = \frac{[CH_4]_{in} - [CH_4]_{out}}{[CH_4]_{in}} \times 100 \quad (3)$$

$$X_{CO_2} = \frac{[CO_2]_{in} - [CO_2]_{out}}{[CO_2]_{in}} \times 100 \quad (4)$$

where $[CH_4]_{in}$, $[CH_4]_{out}$, $[CO_2]_{in}$ and $[CO_2]_{out}$ are the molar concentration of CH_4 and CO_2 in the feed and effluent, respectively.

3.0 RESULTS AND DISCUSSION

3.1 N_2 physisorption Analysis

The N_2 adsorption-desorption isotherms of the MSN and Ni/MSN catalysts are shown in Figure 1A. According to the IUPAC classification, all samples show a Type IV isotherm, which are characteristic of mesoporous materials [15]. At low relative pressure between 0-0.3, formation of a monolayer of adsorbed molecules in micropores is the prevailing process. At medium relative pressure, the adsorption in mesopores leads to multilayer formation and then condensation take place. At high relative pressure between 0.85-1, a sharp rise of adsorbed molecules was observed, indicating the adsorption in interparticles voids. The isotherms of the sample exhibited H1 type hysteresis loop, which is typical for mesoporous material. The adsorption in micropores decreased with increasing the Ni content, suggesting pore blockage upon the addition of Ni. However, the adsorption in interparticles voids were increased with the addition of Ni up to 10 wt% and decreased at the following Ni loading, evidencing that the 10Ni/MSN has the highest interparticles voids.

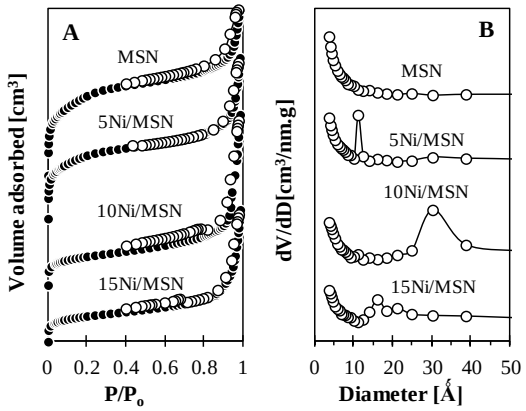

Figure 1 (A) Nitrogen adsorption desorption isotherms and (B) pore size distributions of MSN, 5Ni/MSN, 10 Ni/MSN and 15Ni/MSN

The textural properties of MSN and Ni/MSN catalysts are summarized in Table 1. All Ni/MSN showed lower values of the textural properties compared to those related to the MSN catalyst. The surface area and pore volume of the Ni/MSN catalysts decreased monotonically as the Ni loading increased indicates that the incorporation of Ni into the silica framework and partial pore blockage of pores with Ni particles [16].

Table 1 Textural properties of MSN and Ni/MSN catalysts

Catalysts	Surface area [m^2/g]	Pore volume [cm^3/g]	Pore size [nm]
MSN	868	0.783	3.6
5Ni/MSN	685	0.735	4.3
10Ni/MSN	309	0.761	9.9
15Ni/MSN	275	0.583	8.4

Pore size distribution obtained from the desorption branch of the N_2 isotherm by the BJH method is shown in Figure. 1B. The pore size distribution of MSN is quite narrow in the range 0.5-1 nm and the average pore size is 3.6 nm. The average pore size of 5Ni/MSN, 10Ni/MSN and 15 Ni/MSN catalysts are 4.3, 9.9 and 8.4 nm, respectively. The pore size distribution for Ni/MSN catalyst becomes broader with increasing Ni loading suggesting that some Ni particles located on the external surface generated interparticles voids that increased the average pore size. However, with further increased in Ni loading led to a decrease in pore size which may be due to a blockage of the interparticles pores by the deposition of Ni in large aggregates. This assumption is in agreement with the results shown in

literature, in which reported a decline in surface area due to the partial blockage of the mesopores by large particles deposition [17].

3.2 X-Ray Diffraction Analysis

The XRD patterns of MSN and Ni/MSN catalysts are shown in Figure 2. In the low-angle XRD patterns (Figure 2A), three peaks were observed at 2θ = 2.35, 4.05 and 4.65° corresponding to (100), (110) and (200) planes of a hexagonal lattice, respectively. Although Ni/MSN catalysts exhibit similar diffractions to the MSN, these catalysts show relatively weak and broad diffraction peaks, implying a closure of some of the mesopores by Ni in the catalyst preparation and a decrease in uniformity and ordering in the mesoporous structure. A similar observation was also found in the incorporation of Ni into SBA-15 and mesoporous MCM-41, which implying a decrease in framework order [18].

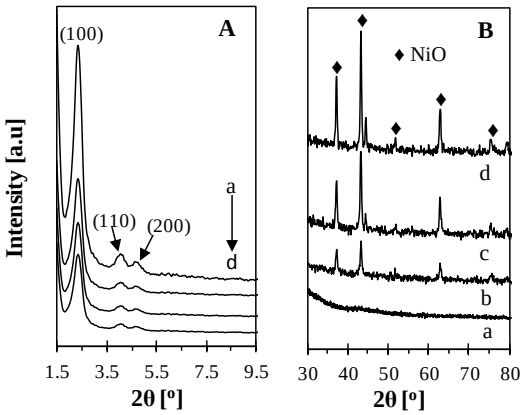

Figure 2 (A) Low and (B) wide XRD patterns of (a) MSN (b) 5Ni/MSN, (c) 10 Ni/MSN and (d) 15Ni/MSN.

Distinctly, there are five new peaks appeared in the wide-angle XRD patterns (Figure 2B) of Ni/MSN catalysts at 2θ = 37.3, 43.3, 51.7, 62.7 and 75.4° which can be definitely ascribed to diffraction of NiO crystals. Increasing the metal loading to 10 wt%, the intensity of NiO peak increases but not very remarkable. Further increasing the Ni loading to 15 wt%, the peak intensity increases significantly, indicating that large Ni crystals are formed. The particles sizes of Ni particle calculated by Scherer formula are shown in Table 2.

Table 2 Ni particle size of Ni/MSN catalysts

Catalysts	Ni particle size [nm]
5Ni/MSN	6.3
10Ni/MSN	8.2
15Ni/MSN	13.5

No remarkable increase of Ni particle size was observed at the metal loading below than 10 wt%, while Ni particle size increased markedly with the further increase of metal loading to 15 wt%. This is suggested that aggregated Ni species may predominate when the Ni loading exceeds the dispersion-limit loading [19].

3.3 FESEM Analysis

The morphological structures of the MSN and 10Ni/MSN catalysts were investigated using FESEM and results are shown in Figure 3. The MSN demonstrated the formation of spherical materials with smooth surface and an average diameter of approximately 100 nm. The introduction of Ni into MSN retained the spherical morphology; however, irregular particles with a rough surface and smaller average diameter at about 80 nm were formed. The deposition of Ni particles in 10Ni/MSN may be contributed to the formation of irregular particles, thus resulted in the formation of interparticles pores.

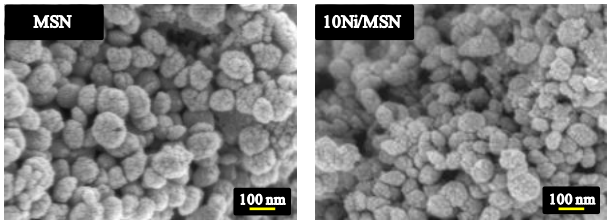

Figure 3 FESEM images of MSN and 10Ni/MSN.

This result is in agreement with the XRD results (Figure 2A) which showed that the incorporation of Ni into MSN led to a slight disruption in the silica framework. A similar phenomenon was reported when ZnO nanoparticles were incorporated in mesostructured silica nanoparticles, which led to a decrease in uniformity and ordering in the mesoporous structure [20].

3.4 Catalytic Testing

The catalytic activities of MSN and Ni/MSN catalysts with different amounts of Ni loadings were evaluated for CO_2 reforming of CH_4 at 700 °C, and results are shown in Figure 4.

A catalytic activity with less than 5 % of CH4 and CO2 conversions was observed for MSN. The presence of 5 wt% Ni loading in MSN promotes the CO2 reforming of CH4, but the promotion is limited due to the lack of enough active sites for the reaction. Further increasing the Ni loading to 10 wt% markedly improves the catalytic activity. However, the CH4 and CO2 conversions were started to decrease by increasing the Ni loading to 15 wt%. The highest conversion reached by 10Ni/MSN is may be closely associated with the optimum amount and dispersion of the Ni active sites available for the reaction.

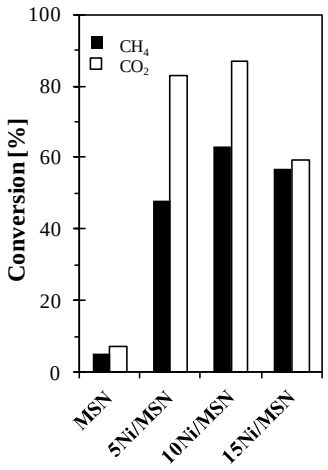

Figure 4 The activity variation during CO_2 reforming of CH_4 at 700 °C over MSN and Ni/MSN catalysts.

Scheme 2 illustrated the nickel dispersion of 10Ni/MSN and 15Ni/MSN catalysts on the surface of MSN. It can be assumed that the improved dispersion of Ni on MSN surface resulted in increase of the interparticles pores, which is consistent with the N_2 adsorption-desorption results. While the lower catalytic activity of 15Ni/MSN is possibly caused by the aggregation of the Ni nanoparticles when the Ni content exceeds the dispersion-limit loading. Metallic Ni species are the active sites for CO_2 reforming of CH_4 [21].

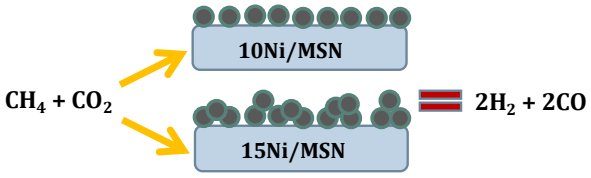

Scheme 2 Schematic illustration of nickel dispersion on 10Ni/MSN and 15Ni/MSN catalysts.

The presence of the larger Ni crystallites on catalyst surface was not beneficial, as it would lead to the fast metal sintering and coke deposition on catalyst [22]. This result is in line with that of XRD results, which showed that increasing Ni loading led to the formation of large Ni crystallites that can lower the Ni dispersion and further affected the catalytic behavior.

4.0 CONCLUSION

In this study, a series (0-15 wt%) of Ni/Mesostructured Silica Nanoparticles (Ni/MSN) were prepared by physical mixing method. The effect of Ni loading on the properties of Ni/MSN catalysts and their performance in CO_2 reforming of CH_4 were investigated. The N_2 adsorption-desorption and XRD results showed that increasing the Ni loading (0-15 wt%) decreased the surface area and crystallinity, and increased Ni particle size in the catalysts, respectively. The activity of the catalysts in CO_2 reforming of CH_4 followed the order of 10Ni/MSN > 15Ni/MSN > 5Ni/MSN > MSN. The results showed that Ni loading gave significant effect on surface area, mesoporous structure and catalytic performance. A balance between Ni particle size and surface area is vital for high CO_2 reforming of CH_4 activity. The highest activity was observed for 10Ni/MSN with the CH_4 and CO_2 conversion of 63.4% and 87.2 %, respectively.

Acknowledgement

The authors would like to express appreciation for the support of the Universiti Teknologi Malaysia through Research University Grant no. 07H06. Our gratitude also goes to the Ministry of Higher Education (MOHE) Malaysia for the award of MyPhD Scholarship (Siti Munirah Sidik) and the Hitachi Scholarship Foundation for the Gas Chromatograph Instrument Grant.

References

[1] Guo, Y. H., Xia, C., Liu, B. S. 2014. Catalytic Properties and Stability of Cubic Mesoporous $La_xNi_yO_z$/KIT-6 Catalysts for CO_2 Reforming of CH_4. *Chem. Eng. J.* 237: 421-429.

[2] Xu, L., Zhao, H., Song, H., Chou, L. 2012. Ordered Mesoporous Alumina Supported Nickel Based Catalysts for Carbon Dioxide Reforming of Methane. *Int. J. Hydrogen Energ.* 37: 7479-7511.

[3] Damyanova, S., Pawelec, B., Arishtirova, K., Fierro, J. L. C., Sener, C., Dogu, T. 2009. MCM-41 Supported PdNi Catalysts for Dry Reforming of Methane. *Appl. Catal. B-Environ.* 92: 250-261.

[4] Ding, R. G. and Yan, Z. F. 2001. Structure Characterization of the Co and Ni Catalysts for Carbon Dioxide Reforming of Methane. *Catal. Today*. 68: 135-143.

[5] de Sousa, F. F., de Sousa, H. S. A., Oliveira, A. C., Junior, M. C. C., Ayala, A. P., Barros, E. B., Viana, B. C., Filho, J.M., Oliveira, A. C. 2012. Nanostructured Ni-containing Spinel Oxides for the Dry Reforming of Methane: Effect of the Presence of Cobalt and Nickel on the Deactivation Behaviour of Catalysts. *Int. J. Hydrogen Energ.* 37: 3201-3212.

[6] Danilova, M. M., Fedorova, Z. A., Zaikovskii, V. I., Porsin, A. V., Kirillov, V.A., Krieger, T.A. 2014. Porous Nickel-based Catalysts for Combined Steam and Carbon Dioxide Reforming of Methane. *Appl. Catal. B-Environ.* 147: 858-863.

[7] Aziz, M. A. A., Jalil, A. A., Triwahyono, S., Saad, M.W.A. 2015. CO_2 methanation over Ni-promoted Mesostructured Silica Nanoparticles: Influence of Ni Loading and Water Vapor on Activity and Response Surface Methodology Studies. *Chem. Eng. J.* 260: 757-764.

[8] Li, Z., Hu, X., Zhang, L., Liu, S., Lu, G. 2012. Steam Reforming of Acetic Acid over Ni/ZrO_2 Catalysts: Effects of Nickel Loading and Particle Size on Product Distribution and Coke Formation. *Appl. Catal. A-Gen.* 417-418: 281-289.

[9] Aziz, M. A. A., Jalil, A. A., Triwahyono, S., Mukhti, R. R., Taufiq-Yap, Y. H., Sazegar, M. R. 2014. Highly Active Ni-promoted Mesostructured Silica Nanoparticles for CO_2 Methanation. *Appl. Catal. B-Environ.* 147: 359-368.

[10] Aziz, M. A. A., Jalil, A. A., Triwahyono, S., Sidik, S. M. 2014. Methanation of Carbon Dioxide on Metal-promoted Mesostructured Silica Nanoparticles. *Appl. Catal. A-Gen.* 486: 115-122.

[11] Karim, A. H., Jalil, A. A., Triwahyono, S., Sidik, S. M., Kamarudin. N. H. N., Jusoh, R., Jusoh, N.W.C., Hameed, B.H. 2012. Amino Modified Mesostructured Silica Nanoparticles for Efficient Adsorption of Methylene Blue. *J. Colloid Interf. Sci.* 386: 307-314.

[12] Jalil, A.A., Kurono, N., Tokuda. M. 2001. Facile Synthesis of 2-arylpropenoic Acid Esters by Cross-coupling using Electrogenerated Highly Reactive Zinc and A Palladium Catalyst. *Synlett*. 12: 1944-1946.

[13] Jalil, A. A., Kurono, N., Tokuda, M. 2002. Facile Synthesis of Ethyl 2-arylpropenoates by Cross-coupling Reaction using Electro-generated Highly Reactive Zinc. *Tetrahedron*. 58: 7477-7484.

[14] Jalil, A. A., Kurono, N., Tokuda. M. 2002. Synthesis of the Precursor of Anti-inflammatory Agents by Cross-coupling using Electrogenerated Highly Reactive Zinc. *Synthesis*. 18: 2681-2686.

[15] Kamarudin, N. H. N., Jalil, A. A., Triwahyono, S., Salleh, N. F. M., Karim, A.H., Mukhti, R.R., Hameed, B.H., Ahmad. A. 2013. Role of 3-aminopropyltriethoxysilane in the Preparation of Mesoporous Silica Nanoparticles for Ibuprofen Delivery: Effect on Physicochemical Properties. *Micropor. Mesopor. Mat.* 180: 235-241.

[16] Li, J. F., Xia, C., Au, C .T., Liu, B. S. 2014. Y_2O_3-promoted NiO/SBA-15 Catalysts Highly Active for CO_2/CH_4 Reforming. *Int. J. Hydrogen Energ.* 39: 10927-10940.

[17] de Sousa, H. S. A., da Silva, A. N., Castro, A. J. R., Campos, A., Filho, J. M., Oliveira, A.C. 2012. Mesoporous Catalysts for Dry Reforming of Methane: Correlation Between Structure and Deactivation Behaviour of Ni-containing Catalysts. *Int. J. Hydrogen Energ.* 37: 12281-12291.

[18] Liu, D., Quek, X. Y., Wah, H. H. A., Zeng, G., Li, Y., Yang, Y. 2009. Carbon Dioxide Reforming of Methane over Nickel-grafted SBA-15 and MCM-41 Catalysts. *Catal. Today*. 148: 243-250.

[19] Liu, D., Lau, R., Borgna, A., Yang, Y. 2009. Carbon Dioxide Reforming of Methane to Synthesis Gas over Ni-MCM-41 Catalysts. *Appl. Catal. A- Gen.* 358: 110-118.

[20] Jusoh, N.W.C., Jalil, A. A., Triwahyono, S., Setiabudi, H.D., Sapawe, N., Satar, M. A. H., Karim, A.H., Kamarudin, N.H.N., Jusoh, R., Jaafar, N.F., Salamun, N., Efendi, J. 2013. Sequential Desilication-isomorphous Substitution Route to Prepare Mesostructured Silica Nanoparticles Loaded with ZnO and Their Photocatalytic Activity. *Appl. Catal. A-Gen.* 468: 276-287.

[21] Huang, T., Huang, W., Huang, J., Ji, P. 2011. Methane Reforming Reaction with Carbon Dioxide over SBA-15 Supported Ni-Mo Bimetallic Catalysts. *Fuel Process. Technol.* 92: 1868-1875.

[22] Fan, M. S., Abdullah, A. Z., Bhatia. S. 2010. Utilization of Greenhouse Gases through Carbon Dioxide Reforming of Methane over Ni-Co/Mgo-ZrO_2: Preparation, Characterization and Activity Studies. *Appl. Catal. B- Environ.* 100: 365-3.